ISSN: 0973-3469, Vol.23, No.(1) 2026, Pg. 20-38

Material Science Research India

www.materialsciencejournal.org

Removal of Chromium from Wastewater Using Carboxymethyl Cellulose Derived from Water Hyacinth

ABU MAHMUD*, LILA DIPTO JOY, MD. HABIBUL ISLAM and SHAMSAD SHARMIN

Department of Materials Science and Engineering, University of Rajshahi, Rajshahi, Bangladesh

Abstract

Water hyacinth (*Pontederia crassipes*), an invasive aquatic weed with severe negative ecological impacts, represents an abundant and low-cost biomass resource due to its high cellulose content. In this study, cellulose was extracted from water hyacinth through degreasing, alkaline treatment, and bleaching, followed by chemical conversion into carboxymethyl cellulose (CMC) via mercerization and etherification. Structural modification was confirmed by FTIR spectroscopy which indicated successful etherification without degradation of the cellulose backbone. X-ray diffraction analysis and morphological examination by SEM of cellulose and CMC showed a clear transformation from well-aligned fibrillar structures in cellulose to a more fragmented, rough, and flaky surface in CMC. Both SEM and X-ray diffraction analysis revealed a pronounced reduction in crystalline order after carboxymethylation, reflecting disruption of the hydrogen-bonded cellulose lattice and increased amorphous character. EDX analysis also revealed a systematic increase in oxygen content consistent with incorporation of oxygen-bearing carboxymethyl groups. Thermogravimetric analysis demonstrated major CMC degradation onset at approximately 250°C suggesting its robust thermal degradation capabilities suited for industrial applications. The synthesized CMC achieved a degree of substitution of 0.69 ± 0.03 (n = 3) indicating a moderate degree of carboxymethyl substitution. From Atomic Absorption Spectroscopy (AAS), a significant decrease in total residual chromium is observed after CMC was introduced and found that CMC can remove 98.69% of total chromium within 30 minutes from water when used at a concentration of 0.75 g/L. Previous works mainly focus on either cellulose or CMC-modified cellulose derived from water hyacinth for water treatment. But here we report the use of CMC extracted from water hyacinth in its nascent form without further chemical modification or composite formation for chromium removal from wastewater for the very first time.

Article History

Received: 06 May 2026

Accepted: 17 June 2026

Keywords

CMC;
Chromium Removal;
Tannery Effluent;
Wastewater;
Water Hyacinth.

CONTACT Abu Mahmud mahmud.matsc@ru.ac.bd Department of Materials Science and Engineering, University of Rajshahi, Rajshahi, Bangladesh

Doi: http://dx.doi.org/10.13005/msri/230104

Abbreviations

CMC	Carboxymethyl Cellulose

Introduction

Water hyacinth is an aquatic plant, found in fresh waters and mud which is scientifically known as *Pontederia crassipes* formerly known as *Eichhornia crassipes*. They can float freely in the freshwater or can stick to mud by their roots. In freshwater, it is invasive as its germination and proliferation rate is high even at low nutrition both as sexually and asexually. Higher salt concentration hinders the growth and reproduction of water hyacinth so it is hardly seen in the coastal areas.[1] The invasive nature of water hyacinth brings various troubles. It makes a dense thick layer on the surface of the water by interlocking the roots which are problematic for the waterway's transportation and making irrigation harder. Besides these, water hyacinth has an impact on the environment as well. Dense water hyacinth mats absorb many nutrients from the ecosystem and block the light going into the water which affects the phytoplankton productivity zooplankton, and reduces the water oxygen level.[1] Imbalance in the aquatic micro-ecosystem, the effect on diversity in fish stock is seen and this creates an optimum situation for the mosquito breeding.[2] To combat such problems created by water hyacinth, various control efforts are applied as mechanical, chemical, biological, and integrated. Besides these, as a rich source of cellulose, water hyacinths can be used as superabsorbent polymer material,[3] heavy metal absorption from water, biogas production etc. Cellulose content differs not only in different anatomical parts of water hyacinth but also water quality and geographical location. However, stems contain the highest amount of cellulose ranging up-to around 60% which makes this aquatic weed a potential source of cellulose.[4] Cellulose is a fibrous, tough, and water-insoluble biopolymer which is generally found in plants with hemicellulose and lignin that imparts mechanical strength to the plants. Moreover, cellulose is a biodegradable, biocompatible, and renewable natural polymer making it an alternative choice to non-degradable fossil fuel-based polymers. Cellulose-based materials have various applications in textiles, cosmetics, water treatment, reinforcing agents, energy storage materials, Pickering emulsion stabilizers, and anti-counterfeiting applications. It also can be used in therapeutic applications such as controlled and sustained drug delivery, wound healing dressing material, transdermal drug delivery, anticancer drug delivery, antimicrobial drug delivery, food packaging and hydrogel production. However, cellulose has some drawbacks too. Due to its strong crystallinity and many hydrogen connections both inside and between molecules, natural cellulose is insoluble in water and various organic solvents, which significantly restricts its applications in wastewater treatment and as biomaterials.[5] For overcoming the drawbacks, cellulose derivatives are developed by esterification, etherification, and oxidation of cellulose in its backbone.[6] Carboxymethyl cellulose (CMC) is a water-soluble,[7] semi-crystalline, non-toxic, biodegradable[8] cellulose derivative containing carboxymethyl groups (-CH_2-COOH). It shows good viscoelastic and rheological properties. It has good properties for film forming and improving the film's overall properties. Various studies showed the actual and potential application of CMC. It has extensive uses in the field of pharmaceuticals, therapeutics, agriculture and in food packaging. CMC is used for the production of superabsorbent hydrogel polymer which has a higher water-absorbing capacity. Besides all of these applications, wastewater treatment with CMC gains special attention as its functional groups can adsorb heavy metals like Cr, Pb and dyes with less or no toxic effects on the aquatic ecosystem. Leather processing industries are one of the major industries in Bangladesh where chromium sulfate is mainly used for leather tanning process which is commonly known as chrome tanning creating health hazards by unsafe disposal of the effluents to the nearby waterbodies and landfills because proper effluent treatment plants (ETP) in tanneries are not yet well established.[9–11] A recent study showed that the average concentration of carcinogenic Cr (VI) in the tannery effluents near Hazaribagh area, Dhaka, Bangladesh is as high as 374.19 ppm,[12] whereas WHO permitted limit of Cr (VI) concentration is only 0.05 ppm in drinking water.[13,14] Discharging these tannery effluent without any treatment makes the soil and water polluted, and sometimes heavy metals enter into the human body via the food chain

creating serious health issues such as cancer, gene alteration, tissue-borne sarcoma, skin diseases etc.[15]

Chemical precipitation, adsorption, bioremediation, ion exchange, membrane filtration, and electro-chemical reduction are the current technologies for Cr (VI) removal from wastewater. Among these, adsorption technique gains special attention because of the applicability of wide range and variation of adsorbents.[16] Various adsorbents employed for Cr (VI) and/or total chromium removal from wastewater as reported in the literature are listed in Table 1. Cellulose, CMC-modified cellulose or metal nano-particle-CMC composites are being tried as adsorbents for heavy metal elimination from water or industrial effluent treatment.[17,18] However, cellulose or CMC-modified adsorbents require more than 90 minutes to remove approximately 95% or more chromium.[19] CMC can be produced from various plant sources.[20] But, considering economic viability and ecological impact, biomass like water hyacinth can be a source of preference for CMC derivation.

Present work reveals that water hyacinth is a safe, feasible and eco-friendly source of cellulose for CMC production, giving sustainable material options while mitigating the environmental complications of this invasive plant species. Though CMC can be derived from other biomass sources, the target of this work is to convert a problematic aquatic weed like water hyacinth into wealth by extracting CMC from it which is then used to solve another problem like cost-effective removal of toxic heavy metals from water. In this article, we applied a comparatively facile route using ethanol to obtain CMC. We investigated total residual chromium elimination ability of extracted CMC from water to figure out its probable potential application for tannery effluent treatment.

Table 1: Various adsorbents employed for Cr (VI) and/or total chromium removal from wastewater as reported in the literature

S.No	Adsorbent	Reduction Efficiency
01	CMC–LDH beads (carboxymethyl cellulose – layered double hydroxide)[21]	96.2%
02	CMC-ZVI (CMC-modified micron zero-valent iron)[22]	>50% (stable after 1 week aging)
03	Water hyacinth activated carbon (phosphoric acid activated, 500°C)[23]	90.4%
04	Water hyacinth cellulose–PVA–PEG membrane[24]	38.75%

Materials and Methods

Materials

Water hyacinth was collected from the various ponds in Rajshahi city, Bangladesh. All chemicals like caustic soda (NaOH), ethanol (C_2H_5OH), monochloroacetic acid ($ClCH_2COOH$), and potassium dichromate ($K_2Cr_2O_7$) are analytical grade reagents from E. Merck, India and were used as such.

Extraction of Cellulose

Cellulose was isolated from *Pontederia crassipes* (water hyacinth) following a modified extraction procedure reported for lignocellulosic biomass and water-hyacinth-derived cellulose materials.[4] For this purpose, roots of collected water hyacinth were eliminated to ease the extraction and leaves along with stems were washed thoroughly with tap water to remove adhered mud and impurities, followed by rinsing with distilled water. These anatomical parts of water hyacinth were selected as the biomass source because of their comparatively high polysaccharide content and ease of chemical processing. The washed biomass was cut into suitable pieces and was sun-dried for 5–7 days until it became visibly dry and suitable for grinding. The dried biomass was then ground using a mixture grinder to obtain a uniform powder. Briefly, 20 g of dried leaves-and-stems powder was taken in a round-bottom flask and treated with 70% ethanol under reflux at 85°C for 120 min to remove extractives such as fats, waxes, and other soluble components. The liquid phase was transferred and the residue washed with 50% ethanol to complete the degreasing process. The pretreated material was subsequently treated with 17.5% NaOH solution at a fiber-to-liquor ratio of 1:20 for 60 min at room temperature with occasional stirring in order to remove hemicellulose. The mixture was filtered and the residue sequentially washed with 5% acetic acid and distilled water until neutral pH was obtained. Delignification was performed by bleaching the residue with 2% sodium hypochlorite (NaOCl) at 30°C for 120 min.[4,25]. After bleaching, the

residue was washed repeatedly with distilled water until the washings became clear and near-neutral pH was reached. At this stage, rich cellulose content was obtained from *Pontederia crassipes* by eliminating hemicellulose and lignin. The extracted cellulose from the biomass source were filtered and dried in an oven at 105°C until constant weights were obtained. The percentage yield of the cellulose was calculated and samples kept in a desiccator for further use in synthesis of CMC. The percentage yield of extracted cellulose was calculated using following equation:

$$\text{Cellulose Yield}(\%) = \frac{\text{Weight of extracted cellulose}}{\text{Initial dry biomass weight}} \times 100$$

Carboxymethyl Cellulose (CMC) Synthesis

The isolated cellulose was converted to carboxymethyl cellulose (CMC) through a mercerization–etherification route adapted from reported CMC synthesis procedures.[26,27] Cellulose fibers were first suspended in 95% ethanol at a solid-to-liquid ratio of 1:20 in a covered round-bottom flask. After 30 min, 40% NaOH solution[28] was added and stirred vigorously for 30 min at room temperature to form alkali cellulose through the alkalization (mercerization) reaction.[26] Etherification was then carried out by dropwise addition of monochloroacetic acid (MCA) at 55°C. The molar ratio of cellulose:MCA was maintained 1:1.2, and the reaction pH was controlled between 8.0 and 9.5 during MCA addition. The mixture was stirred for 3 h to complete the etherification reaction.[26] After cooling, the mixture was filtered to separate the solid phase. The residue was suspended in methanol/water (70/30) and neutralized using 95% acetic acid. The product was washed 5 times with ethanol/water (70/30 v/v) and dried at 60°C in an oven until constant weight was obtained and then stored in a desiccator. The derived CMC was characterized using the following parameters: FTIR, TGA-DTA, XRD, SEM-EDX and degree of substitution. The percentage yield of CMC was calculated by means of following equation:

$$\text{CMC Yield}(\%) = \frac{\text{Weight of dried CMC}}{\text{Weight of cellulose used}} \times 100$$

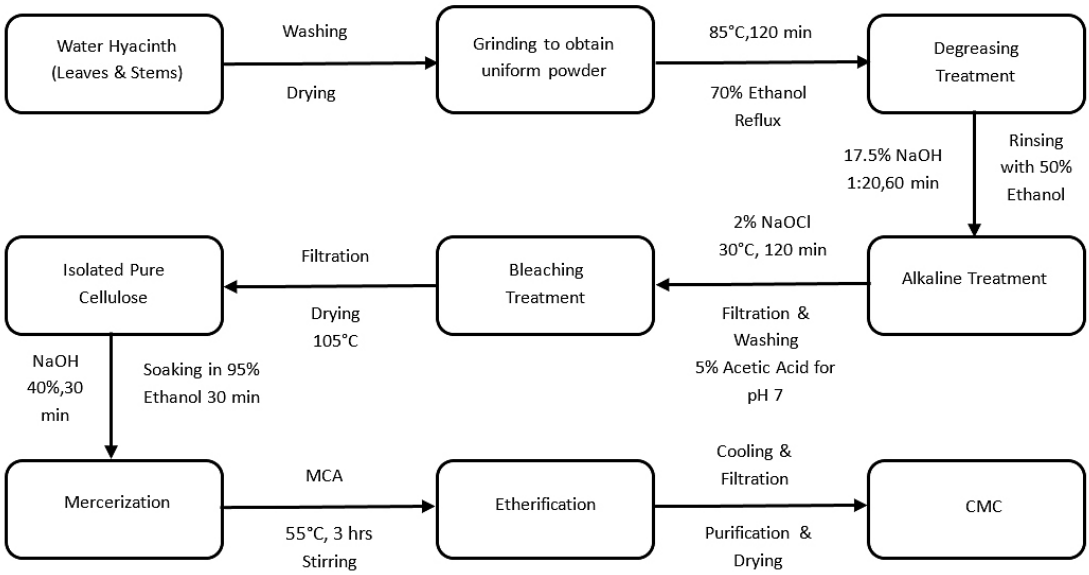

Fig. 1: Flow-chart of CMC derivation from water hyacinth

FTIR Spectroscopy

Using an oven, the samples were dried for 2 hours at 80°C. About 0.5 mg of sample and 100 mg of KBr were mixed and ground finely and heated at the same temperature for 6 hours. Then the blend was compressed to form a pellet. The infrared spectra were recorded with FTIR (Model: Perkin Elmer Spectrum 100, UK) between 400 and 4000 cm^{-1}.

Thermogravimetric Analysis

Thermal analysis was carried out by 'Perkin Elmer STA8000 (USA)'. Readings were taken from room temperature to 800°C. In this process, the temperature change of 10°C/minute was maintained. 5mg samples were taken in an alumina crucible. Dry inert argon gas flowed into the chamber.

XRD Analysis

This analysis of the crystal nature of the sample was done using a LabX XRD-6100 (SHIMADZU X-ray diffractometer). The continuous scan was operated by Cu Kα radiation (λ = 1.5406 Å) in the 2θ range of 10°–60° at a scanning rate of 2°min^{-1}. The XRD instrument was operated at 40 kV and 30 mA. The crystallinity index (CI) of cellulose and CMC was determined using the X-ray diffraction peak deconvolution (peak fitting) method.[29] In this approach, the diffraction pattern was deconvoluted into crystalline and amorphous contributions using OriginPro 2024 software (64-bit, version 10.1.0.178). Gaussian peak functions were used throughout, the initial peak positions were manually assigned, and the fitting model was iteratively optimized until the best fit was achieved based on the maximum R^2 (coefficient of determination, COD) values. To maintain internal consistency, the same 2θ interval (10°–60°) was used for peak fitting, fitted-peak area determination, and total area integration. The crystallinity index (CI) was calculated by an area-based deconvolution method[30] according to:

$$\mathbf{CI}(\%) = \frac{\mathbf{A_c}}{\mathbf{A_t}} \times \mathbf{100}$$

Where, A_c is the summed area of the selected crystalline peaks obtained from Gaussian deconvolution, and A_t is the total integrated area of the baseline-corrected diffraction profile within the same 2θ range (10°–60°), determined using the Analysis–Mathematics–Integrate function in OriginPro. This treatment is consistent with area-based XRD deconvolution approaches in which the crystalline fraction is defined from the ratio of crystalline peak area to total pattern area, while whole-pattern methods that account for both crystalline and amorphous contributions are generally considered more reliable than simple peak-height methods for cellulose crystallinity assessment.[29]

SEM-EDX Analysis

Surface morphology of both cellulose and carboxymethyl cellulose (CMC) was examined using an ultra-high-resolution field-emission scanning electron microscope (SEM, JSM-7610F, JEOL, Japan). Prior to imaging, the samples were sputter-coated with platinum using a JEOL Auto Fine Coater (JEC-3000FC) to improve conductivity.

The elemental composition of cellulose was analyzed by energy-dispersive X-ray spectroscopy (EDX) attached to the same (SEM, JSM-7610F, JEOL, Japan) machine, while the elemental composition of CMC was determined using EDX coupled with a JEOL JCM-6000Plus NeoScope scanning electron microscope (SEM) (JEOL Ltd., Japan). Though the machines for EDX analysis were different for cellulose and CMC, conducting platinum coating were applied for both of the samples. The results were reported as weight percentage (wt%) and atomic percentage (at%).

Degree of Substitution (DS)

The degree of substitution (DS) of CMC was determined using an acid-wash/back-titration procedure based on ASTM D1439-03 Test Method A.[31] Approximately 4 g of CMC was transferred into a 250 mL beaker and mixed with 75 mL of 95% ethanol to obtain a uniform slurry. While stirring, 5 mL of nitric acid was added, and the slurry was further agitated, heated, and boiled briefly to convert the water-soluble CMC into the insoluble acid form. The supernatant was decanted, and the precipitated acid carboxymethyl cellulose was washed with hot 80% ethanol until nitrate was no longer detected by the diphenylamine reagent test. After cooling in a desiccator, the sample was washed with anhydrous methanol and dehydrated at 105°C.

For the back-titration step, 1.15 g of the dried acid carboxymethyl cellulose was transferred into a 500 mL Erlenmeyer flask, and 100 mL of distilled water was added. Subsequently, 25.00 mL of 0.5 N NaOH was introduced with stirring, and the mixture was heated to boiling and maintained for 15 min to reconvert the acid form into the sodium form. The excess alkali was then titrated while hot with 0.3 N HCl using phenolphthalein as the indicator until the endpoint was reached. The determination was carried out in triplicate.

The degree of substitution was calculated using the following equation:

$$\mathbf{A} = \frac{\mathbf{BC} - \mathbf{DE}}{\mathbf{F}}$$

$$\textbf{Degree of substitution}(\mathbf{DS}) = \frac{\mathbf{0.162A}}{\mathbf{1} - (\mathbf{0.058A})}$$

Where,
A is the milliequivalents of acid spent per gram of sample, B is the volume of NaOH solution required (mL), C is the normality of NaOH, D is the volume of HCl needed for back-titration (mL), E is the normality of HCl, and F is the mass of acid carboxymethyl cellulose used (g).[31]

Atomic Absorption Spectroscopy (AAS)

Atomic Absorption Spectroscopy (AAS) was employed to determine the residual chromium concentration in the filtrates obtained after treatment with carboxymethyl cellulose (CMC). The measurements were carried out using a Shimadzu AA-6800 atomic absorption spectrophotometer.

In the present experiment, chromium-containing solutions were prepared using potassium dichromate ($K_2Cr_2O_7$) as the chromium source. At first, approximately 100 ppm of chromium containing stock solution was prepared by dissolving 0.283 g of dried reagent grade $K_2Cr_2O_7$ in 1000 mL distilled water. From this stock solution, 1000 mL approximately 0.06 ppm chromium solution (above the WHO drinking water guideline) was made by sequential dilution. From this solution, four 200 mL aliquots were taken. One aliquot was kept as a blank without adding CMC, while 0.05 g, 0.10 g, and 0.15 g of CMC were added to the remaining three aliquots, corresponding to 250, 500, and 750 mg/L of CMC in the solution. The pH of the blank chromium solution was 5.6, while the pH values of the suspensions containing 250, 500, and 750 mg/L CMC were 5.3, 5.1, and 5.0, respectively. The suspensions were stirred for 30 minutes at room temperature to allow interaction between chromium species and the CMC. After stirring, all solutions were filtered using Whatman Grade 602h filter paper to remove the suspended adsorbent particles. The filtrates were subsequently analyzed by AAS to determine the residual chromium concentration in the aqueous phase after treatment. Each measurement was performed in triplicate to ensure precision. It is important to note that AAS determines chromium as an element in the analyzed solution; therefore, direct oxidation-state specific quantification of Cr (VI) requires additional separation or speciation procedures prior to AAS analysis. Since such a speciation protocol was not included in the present analytical procedure, the AAS measurements in this study are interpreted as residual chromium concentration in the filtrate. The chromium removal efficacy was calculated by means of the following equation:

$$\textbf{Removal}\ (\%) = \frac{\mathbf{C_0} - \mathbf{C_e}}{\mathbf{C_0}} \times \mathbf{100}$$

where (C_0) signifies the initial chromium concentration (blank value) and (C_e) represents the residual chromium concentration after treatment.

Results and Discussion

Results

The average yield% of cellulose is 33.33±2.20% while the yield% of synthesized CMC obtained in this work was 62.7% corresponding to the experimental batch used in this study from water hyacinth leaves along with stems. The FTIR spectroscopic analysis of cellulose and CMC confirms that cellulose was successfully converted into carboxymethyl cellulose. The comparative XRD results of cellulose and CMC showed that the conversion of cellulose to CMC is associated with reduced crystalline order and enhanced amorphous character. Thermogravimetric analysis demonstrated major CMC degradation onset at approximately 250°C. SEM analysis revealed a pronounced reduction in crystalline order of cellulose after carboxymethylation, reflecting disruption of the hydrogen-bonded cellulose lattice and increased amorphous character in CMC. The comparative EDX analysis revealed a systematic increase in oxygen content in CMC which is consistent with incorporation of oxygen-bearing carboxymethyl groups during carboxymethylation. The degree of substitution (mean DS= 0.69 ± 0.03) value indicates a successful introduction of carboxymethyl groups during etherification. From Atomic Absorption Spectroscopy (AAS), it was found that CMC can remove 98.69% of total chromium within 30 minutes from wastewater when used at a concentration of 0.75 g/L.

Discussion

Extraction of Cellulose and CMC Synthesis

The cellulose yield% is consistent with previously reported cellulose extraction yields from lignocellulosic biomass, where values typically range from 25–40% depending on plant source and treatment conditions. The extracted cellulose was subsequently converted to CMC (Figure 2) using an alkalization-etherification process. A 40% NaOH concentration was used during mercerization to activate the cellulose structure and promote formation of alkali cellulose, which facilitates nucleophilic substitution during the etherification step. The yield% of CMC indicates efficient conversion of cellulose to the etherified derivative. During the etherification reaction, monochloroacetic acid was added dropwise while maintaining the pH between 8 and 9.5, ensuring controlled substitution of hydroxyl groups in the cellulose backbone. Such reaction conditions promote formation of carboxymethyl groups at the accessible hydroxyl sites of cellulose without excessive side reactions.

Fig. 2: Extracted Cellulose & CMC

FTIR Spectroscopy

The FTIR spectrum of cellulose isolated from water hyacinth (Figure 3) shows characteristic absorption bands consistent with pure cellulose. A broad band centered at 3436 cm^{-1} is attributed to O–H stretching vibrations coming from strong intra- and intermolecular hydrogen bonding within the cellulose macromolecular structure.[32] The absorption band at 2918 cm^{-1} is attributed to C–H stretching vibrations of aliphatic –CH and –CH_2 groups in the glucopyranose units of cellulose. The band observed at 1634 cm^{-1} is assigned to H–O–H bending vibrations of physically adsorbed water, which is commonly reported for hydrophilic cellulose materials. Peaks appearing at 1384 cm^{-1} and within the 1161–1060 cm^{-1} region are attributed to C–H bending and C–O–C/C–O stretching vibrations of β-(1→4)-glycosidic linkages, confirming that the cellulose backbone remains intact after extraction. A weak band at around 559 cm^{-1} in the fingerprint region was also observed in the cellulose spectrum which represents the bending vibrations of C-C-O and C-O-C groups. After carboxymethylation, the FTIR spectrum of carboxymethyl cellulose (CMC) exhibits clear spectral modifications. The O–H stretching band shifts from 3436 cm^{-1} to lower wavenumbers (~3118 cm^{-1}), indicating alteration of the hydrogen-bonding environment due to substitution of hydroxyl groups by carboxymethyl functionalities.[26,33] A distinct absorption band appearing at 1623 cm^{-1} is attributed to the asymmetric stretching vibration of carboxymethyl carboxyl groups (–COO^-/–COOH). Absorption bands in the range of 1600–1640 cm^{-1} have been consistently reported as a diagnostic feature of carboxymethyl cellulose and absence of an ester carbonyl peak (~1740 cm^{-1}), confirming

successful etherification of the cellulose backbone.[26] The accompanying band near 1382 cm^{-1} corresponds to symmetric stretching and deformation modes of carboxymethyl groups, providing further evidence of carboxymethyl substitution. The coexistence of characteristic cellulose skeletal vibrations with newly formed carboxymethyl-related bands confirms that cellulose was successfully converted into carboxymethyl cellulose without degradation of its polymer backbone.

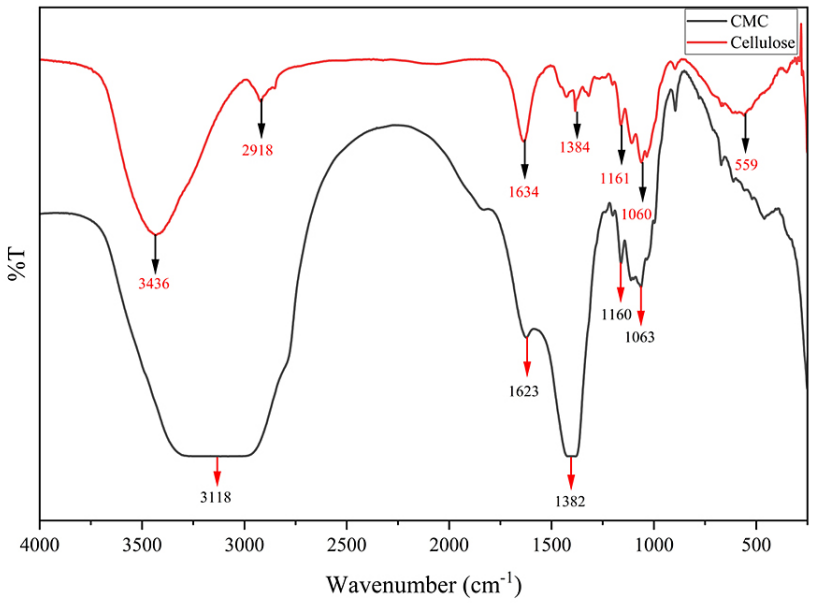

Fig. 3: FTIR analysis of cellulose and CMC

XRD Analysis

XRD analysis (Figure 4) of cellulose shows sharper and better-defined reflections than CMC, indicating a higher degree of structural order, while the CMC profile is broader and more diffuse, consistent with reduced long-range order after etherification. The X-ray diffraction (XRD) pattern of cellulose exhibits the characteristic features of a semi-crystalline polymeric material. A dominant diffraction peak is observed in the 2θ range of approximately 20–23°, which is commonly associated with the crystalline domains of native cellulose, along with weaker reflections at lower diffraction angles and this clear and sharper peak in this region is also suggestive of the elimination of lignin and hemicellulose.[25] In addition to these crystalline features, a broad diffuse background is present, indicating the coexistence of amorphous regions within the cellulose matrix.[34] Such diffraction behavior is well documented for cellulose materials and reflects the partial ordering of cellulose chains stabilized by an extensive inter- and intramolecular hydrogen-bonding network.[34] Moreover, for cellulose, the peaks at 15.5°, 22.30°, and 34.64° were assigned to the characteristic cellulose I reflections. These are in good agreement with established cellulose I diffraction descriptions and with experimentally reported cellulose peaks near 15.7°, 22.6°, and 35.19° assigned to the (110), (200), and (004) planes, respectively.[35,36] Because the XRD pattern of cellulose in the present work was collected before the 40% NaOH mercerization step, the cellulose diffractogram is appropriately interpreted as cellulose I rather than mercerized cellulose II. In contrast, the XRD pattern of carboxymethyl cellulose (CMC) (Figure 4) shows clear structural modifications relative to the parent cellulose. The principal diffraction feature centered around 2θ ≈ 20–22° becomes noticeably broader and less well defined, accompanied by an overall increase in diffuse scattering intensity. This reduction in peak sharpness and enhancement of the amorphous contribution indicate a decrease in long-range

crystalline order following chemical modification of cellulose.[27,33] Similar diffraction characteristics have been widely reported for CMC and other cellulose ether derivatives produced through etherification reactions.[27,34] To quantitatively evaluate this structural transformation, the crystallinity index (CI) was calculated from the XRD patterns using the X-ray diffraction peak deconvolution (peak fitting) method.[29,30] Based on this calculation, the crystallinity index of cellulose was found to be 69.00% whereas the crystallinity index of CMC decreased to 43.39%, indicating a reduction in structural order after carboxymethylation. The decrease in crystallinity observed after carboxymethylation can be ascribed to the replacement of hydroxyl groups along the cellulose backbone by carboxymethyl groups, which dislocates the inter- and intramolecular hydrogen-bonding network responsible for maintaining the native cellulose crystalline lattice. As a result, the regular packing of cellulose chains is hindered, leading to an increase in amorphous regions within the polymer structure.[33] A similar reduction in crystallinity has also been reported for cellulose obtained from various biomass sources. For example, cellulose fibers isolated from rice husk exhibit typical semi-crystalline diffraction patterns and structural characteristics consistent with native cellulose materials.[34] Likewise, CMC synthesized from banana pseudostem cellulose has been reported to show decreased crystallinity after etherification reactions due to disruption of the ordered hydrogen-bonded structure of cellulose chains.[27] These literature observations support the trend observed in the present study, where the crystallinity index decreased from 69.00% in cellulose to 43.39% in CMC, confirming that carboxymethylation leads to partial loss of crystalline order and increased amorphous character in the modified polymer matrix. Overall, the comparative XRD results demonstrate that the conversion of cellulose to CMC is associated with reduced crystalline order and enhanced amorphous character, which is consistent with structural changes expected from chemical substitution of the cellulose framework.[34]

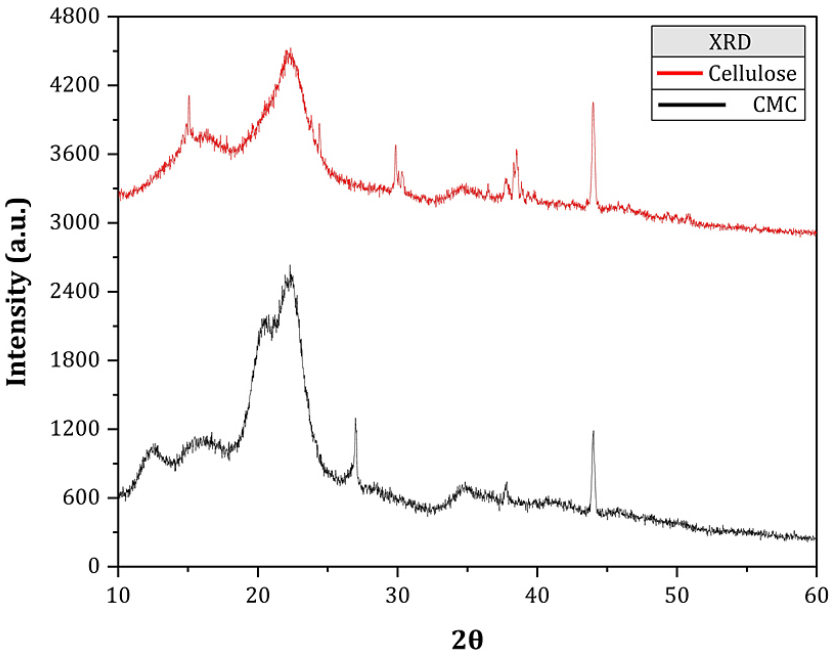

Fig. 4: XRD analysis of cellulose & CMC

Thermogravimetric Analysis

The thermogravimetric (TGA) and differential thermal analysis (DTA) profiles of cellulose and carboxymethyl cellulose (CMC) (Figure 5 and 6) exhibit distinct multi-stage thermal degradation behaviors, reflecting changes in thermal stability

induced by chemical modification of the cellulose backbone. For cellulose, an initial weight loss of approximately 8.85% is observed below ~120°C, which is attributed to the evaporation of physically adsorbed and weakly bound moisture, as confirmed by a corresponding low-temperature endothermic signal in the DTA curve. A subsequent minor mass loss of about 13.5% occurs up to ~300 °C, followed by the principal degradation stage between ~300 and 380°C, accounting for approximately 51.52% weight loss. This dominant decomposition event is associated with depolymerization and thermal cleavage of the cellulose backbone through the breakdown of glycosidic linkages.[37] At temperatures above 400°C, a gradual mass loss of around 12.49% is observed, corresponding to the slow degradation of carbonaceous char residues. The total weight loss of cellulose reaches approximately 86.36% at 800 °C, which is consistent with the thermal behavior reported for native cellulose materials.[37] In comparison, CMC exhibits a modified degradation profile with reduced thermal stability. An initial mass loss of approximately 8.34% below ~150°C is similarly attributed to moisture removal.[33] The primary degradation step occurs at lower temperatures, with a major weight loss of about 61.38% between ~250 and 350°C, indicating an earlier onset of thermal decomposition relative to cellulose. Such a shift toward lower decomposition temperatures and multi-step mass-loss behavior is consistent with reported thermogravimetric studies of CMC, where carboxymethyl substitution alters the thermal scission pathway and reduces thermal resistance relative to native cellulose.[38] Additional degradation stages of approximately 14.64% and 10.68% are observed at higher temperatures, which can be credited to progressive decomposition of the chemically substituted polymer backbone and residual structures. The overall mass loss of CMC reaches approximately 95.04% at 800°C, indicating lower char formation compared to cellulose, a behavior also commonly observed in thermal degradation studies of CMC and its salt forms.[38] Overall, the downward shift in degradation temperatures and the increased mass loss observed for CMC confirm altered thermal behavior following carboxymethylation. This behavior is consistent with disruption of the hydrogen-bonded cellulose network caused by substitution of hydroxyl groups with carboxymethyl moieties, resulting in reduced structural integrity and thermal stability.[33,38]

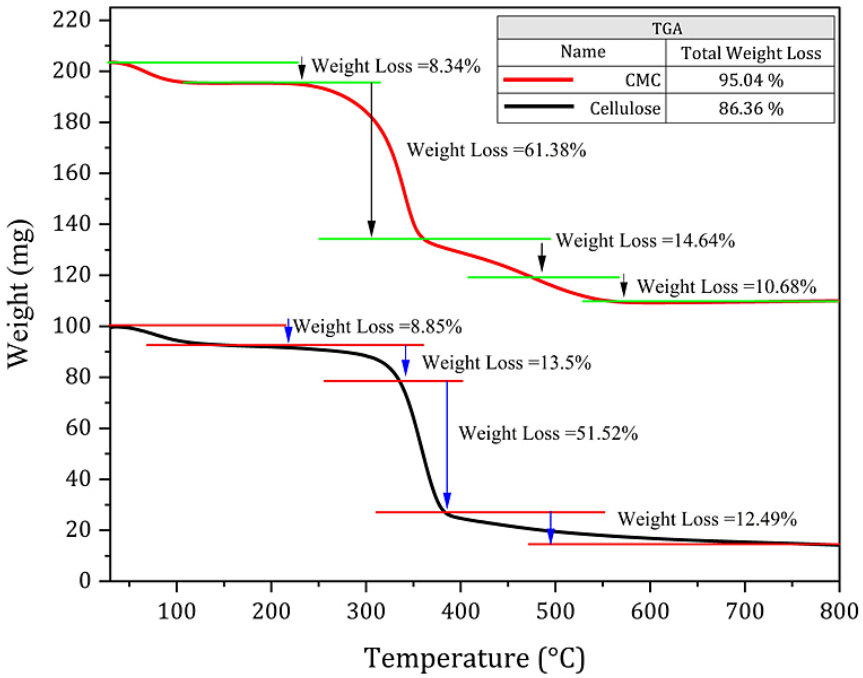

Fig. 5: TGA analysis of cellulose & CMC

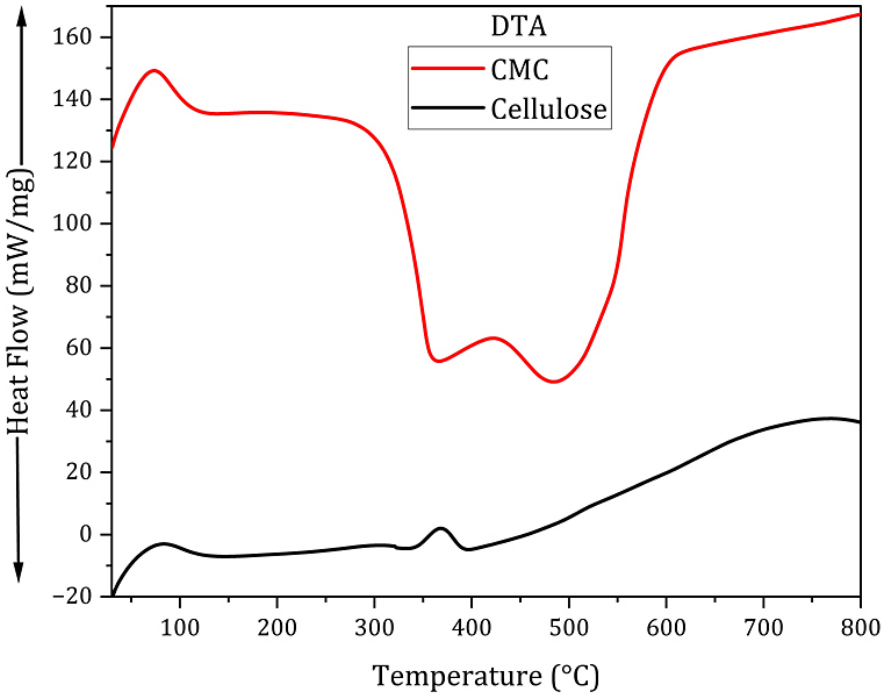

Fig. 6: DTA analysis of cellulose & CMC

Morphological Analysis

The surface morphology of cellulose and carboxymethyl cellulose (CMC) was examined using scanning electron microscopy to observe structural changes caused by carboxymethylation. The SEM micrograph of cellulose (Figure 7) shows well-defined fibrillar structures with elongated microfibrils arranged along the fiber direction. These ribbon-like fibrillar bundles extend over several micrometers and are clearly visible with reference to the 5 µm scale bar, indicating that the extracted cellulose retains the typical hierarchical microfibrillar organization commonly reported for purified cellulose fibers. The presence of aligned fibrillar structures suggests that the native cellulose framework remains largely intact after the extraction and purification steps. In contrast, the SEM micrograph of CMC (Figure 8) reveals a distinctly different morphology compared with the parent cellulose. The ordered fibrillar network observed in cellulose is no longer visible, and the surface is instead composed of irregular fragmented and flaky structures. With reference to the 1 µm scale bar, these fragments appear predominantly within the sub-micrometer to micrometer size range. The disappearance of continuous fibrillar bundles and the formation of collapsed surface structures indicate that the chemical modification process has disrupted the original microfibrillar arrangement of cellulose. Such morphological changes are consistent with the introduction of carboxymethyl groups into the cellulose backbone during etherification, which weakens the inter- and intramolecular hydrogen bonding responsible for maintaining the ordered cellulose structure.[39] As a result, the cellulose chains become more disordered and the microfibrillar integrity is reduced, leading to the irregular and fragmented morphology observed in the CMC micrograph. Overall, the SEM observations demonstrate a clear transition from a micrometer-scale fibrillar structure in cellulose (Figure 7) to a fragmented sub-micrometer to micrometer-scale morphology in CMC (Figure 8), providing visual evidence of structural modification following carboxymethylation.[39] Overall, the SEM observations indicate a qualitative morphological transition from a more ordered fibrillar structure in cellulose to a more fragmented and flakier surface in CMC after carboxymethylation. The comparison presented here is interpreted qualitatively on the basis of the observed surface features.

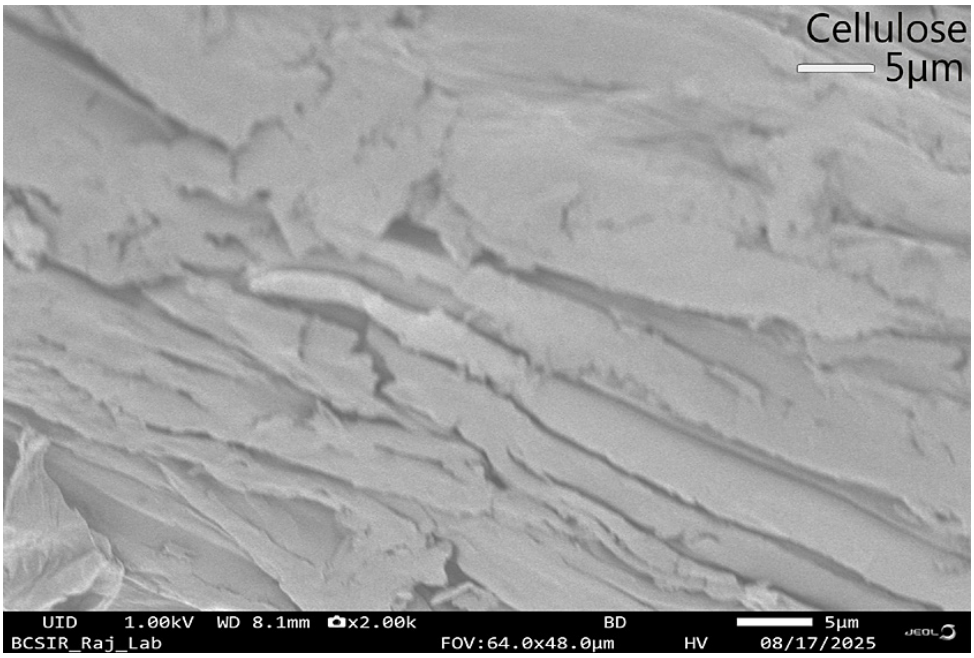

Fig. 7: SEM analysis of cellulose

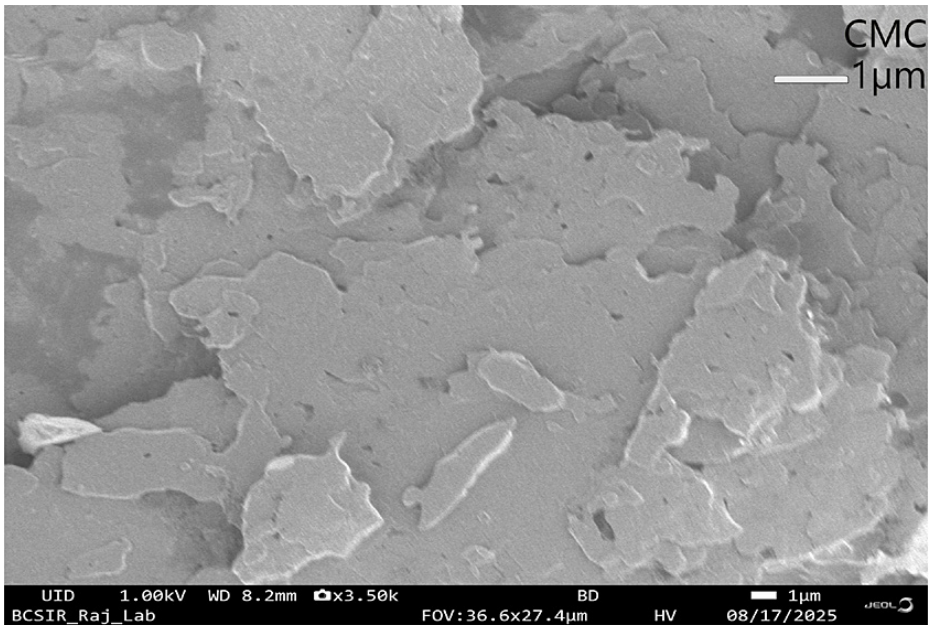

Fig. 8: SEM analysis of CMC

Energy-dispersive X-ray (EDX) Analysis

Energy-dispersive X-ray (EDX) spectroscopy was used to evaluate the near-surface elemental composition of water hyacinth–derived cellulose and its carboxymethylated product (CMC), in order to capture elemental-level trends associated with purification and etherification. The EDX spectrum of the extracted cellulose (Figure 9) is dominated by the characteristic C Kα (~0.27 keV) and O Kα (~0.51 keV) signals, which is typical of cellulose-rich

polysaccharides and is widely reported for purified cellulosic substrates characterized by SEM–EDX/EDX methods.[39] In the present sample, cellulose contains 47.96 wt% C (55.13 at%) and 52.04 wt% O (44.87 at%), consistent with the oxygen-rich elemental profile commonly observed for cellulose after effective removal of non-cellulosic fractions.[39] After carboxymethylation, the spectrum remains governed by carbon and oxygen peaks, indicating that the polysaccharide backbone is preserved following chemical modification.[39] However, The EDX spectrum of CMC shows (Figure 10) the elemental distribution shifts markedly. Carbon content decreases to 38.8 wt% (45.79 at%) while oxygen increases to 61.2 wt% (54.21 at%). Such oxygen enrichment is chemically consistent with incorporation of oxygen-bearing carboxymethyl substituents ($–CH_2–COO^-$) onto cellulose hydroxyl groups during etherification, and analogous oxygen-increase trends have been reported in EDX-supported studies of CMC and CMC salts/derivatives.[38] As EDX spectra of cellulose and CMC were acquired using different instruments and operating conditions, the elemental comparison presented here is interpreted as semi-quantitative rather than as a strictly direct quantitative comparison[40,41] and thus the observed C/O shift is therefore discussed as a compositional trend consistent with carboxymethylation, not as definitive evidence of bulk composition. No detectable Na signal was observed in the CMC spectrum. Although concentrated NaOH was used during mercerization, the product was subsequently neutralized with acetic acid and repeatedly washed until near-neutral pH was reached, which would be expected to reduce residual sodium and associated inorganic species at the analyzed surface.[26] In addition, EDX is surface-sensitive, and the detection of low atomic number elements depends strongly on concentration, matrix, and analytical conditions; therefore, residual sodium present at low concentration or outside the analyzed near-surface region may remain undetected.[38,39] It is also noteworthy that when sodium is present as a sufficiently abundant counter-ion in CMC salts, EDX can reveal the corresponding cation signal.[36] Accordingly, the absence of a visible Na peak in the present CMC spectrum is interpreted as the combined consequence of purification and the intrinsic detection limitations of EDX, rather than as definitive proof of complete sodium removal. It should also be noted that EDX analysis of organic specimens may be affected by hydrocarbon contamination under electron irradiation, which can contribute uncertainty to the apparent carbon signal.[40] Accordingly, the present EDX results are best interpreted as near-surface, semi-quantitative compositional evidence supporting successful carboxymethylation of cellulose.

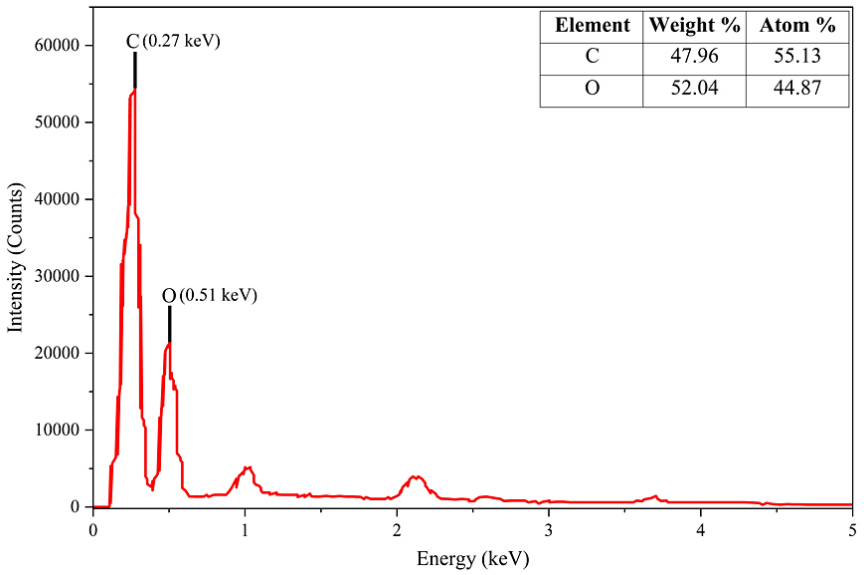

Fig. 9: EDX analysis of Cellulose

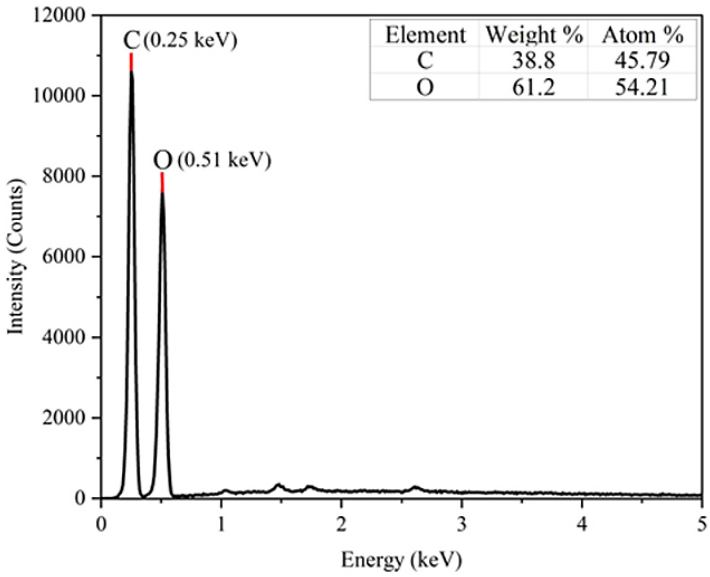

Fig.10: EDX analysis of CMC

Degree of Substitution (DS)

The degree of substitution (DS) represents the average number of hydroxyl groups in the cellulose backbone that are replaced by carboxymethyl groups during the etherification reaction.[27] In the cellulose molecule, the hydroxyl groups located at the C2, C3, and C6 positions can potentially be substituted; therefore, the theoretical maximum DS value for cellulose derivatives is 3, although practical DS values are typically much lower due to steric and reaction limitations.[27] The triplicate back-titration required 28.9, 28.6, and 28.1 mL of 0.3 N HCl, which corresponded to DS values of 0.67, 0.69, and 0.72, respectively, giving a mean DS of 0.69 ± 0.03 (n = 3). The obtained DS value indicates a moderate degree of substitution within the cellulose structure and confirms successful introduction of carboxymethyl groups during etherification.[26,27] Reported DS values for laboratory-synthesized CMC commonly fall within the range of approximately 0.4 to 1.0 depending on alkali concentration, etherifying agent dosage, reaction temperature, and reaction time.[26,27] The value obtained in the present work therefore lies within the range generally reported for biomass-derived CMC materials and supports effective chemical modification of water hyacinth cellulose.[26,27]

Native cellulose contains extensive intra- and intermolecular hydrogen bonding, which makes it practically insoluble in water. The inclusion of carboxymethyl groups interrupts this hydrogen-bonding network and increases the hydrophilicity of the polymer chain, thereby enhancing its interaction with water molecules.[26,27] However, because solubility was not directly quantified in the present study, the DS value is interpreted here as an indicator of the extent of carboxymethyl substitution rather than as direct evidence of solubility.[26,27] This interpretation is consistent with the FTIR, XRD, and SEM–EDX results, which collectively support successful conversion of cellulose into carboxymethyl cellulose.

Atomic Absorption Spectroscopy (AAS)

The removal capability of the CMC sample toward chromium ions was evaluated visually and by measuring the residual chromium concentration in the blank and CMC-treated solutions using AAS. As shown in Figure 11, a substantial decrease in chromium concentration was observed after the addition of CMC to the chromium-containing solution. The blank filtrate showed a chromium concentration of 0.0609 ppm, whereas the filtrates obtained after treatment with 250, 500, and 750 mg/L CMC showed chromium concentrations of 0.0068 ppm, 0.0042 ppm, and 0.0008 ppm, respectively. The progressive reduction in chromium concentration with increasing CMC dosage indicates that a higher dose leads to greater removal of dissolved chromium from the solution. The removal efficiencies were 88.83%,

93.10%, and 98.69% for 250, 500, and 750 mg/L CMC, respectively. These results validate that increasing the amount of CMC significantly reduces the measured chromium concentration in the solution under the experimental conditions applied. CMC is a cellulose-derived polymer containing abundant hydroxyl (–OH) and carboxymethyl (–COOH/–COO^-) functional groups, which can interact with dissolved metal species through various physicochemical interactions in aqueous media like electrostatic attractions, coordination and hydrogen bonding.[42–44] It should be mentioned that the current study was directed under a single fixed contact time of 30 minutes, and no systematic investigation of adsorption kinetics, equilibrium isotherms, or pH-dependent chromium speciation was performed. The adsorption behavior of chromium is strongly influenced by the aqueous speciation of Cr (VI), which can exist as $HCrO_4^-$, CrO_4^{2-}, or $Cr_2O_7^{2-}$ depending on solution pH and concentration.[43] However, the gradual pH decrease observed after CMC addition, from 5.6 in the blank solution to 5.3, 5.1, and 5.0 in the treated suspensions, indicates that the solution chemistry changed systematically with increasing CMC dosage. Because chromium speciation in water is strongly pH-dependent, the behavior of chromium in the present system may have been influenced not only by CMC dosage but also by the acidic-to-mildly acidic pH range of the medium.[42,45] Under such conditions, pH-dependent chromium speciation and possible Cr(VI)/Cr(III)-related transformation leading to in-situ reduction and complexation with CMC cannot be ruled out completely.[45,46]

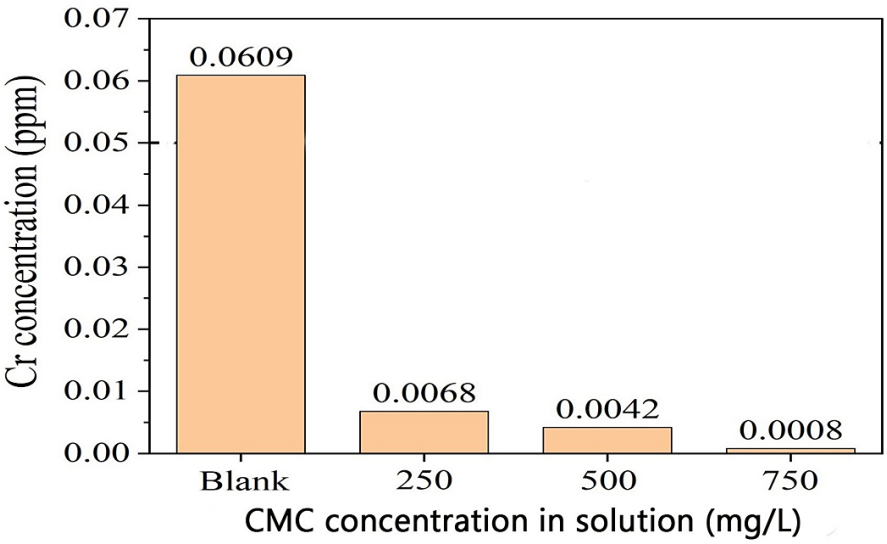

Fig. 11: Concentration changes of chromium in water after treatment with CMC

At the same time, the present experimental design involved treatment of the chromium-containing solution with a water-soluble CMC system followed by filtration. Therefore, although the measured chromium concentration in the filtrate decreased markedly with increasing CMC dosage, the present data do not by themselves establish a single, definitive adsorption pathway. Instead, CMC-chromium complexes, CMC gel particles, or CMC aggregates may be physically retained by the filter, producing a reduction in filtrate chromium that reflects co-filtration rather than surface adsorption. This interpretation is particularly relevant because the suspensions were filtered (by Whatman Grade 602h filter paper) prior to AAS analysis and the AAS result reflects only the residual chromium concentration in the filtrate.

However, as the pH of the solution was not systematically controlled or investigated in this study, no mechanistic interpretation regarding the adsorption pathway of chromium species onto the CMC surface or co-filtration mechanism is proposed here. Therefore, the present results should be

interpreted as preliminary screening evidence demonstrating that increasing the dose of CMC reduces the residual chromium concentration in the filtrate under the tested experimental condition. In addition, the recovery or regeneration of the spent CMC phase was not investigated in the present study, and this remains an important aspect for future practical evaluation of the material in wastewater treatment applications

Conclusion

Water hyacinth, an aquatic weed with a higher proliferation rate causes various problems to the aquatic ecosystem and waterways. This weed was used to produce CMC, a water-soluble derivative of cellulose, through alkaline treatment mercerisation and etherification. This derived CMC was tried for residual chromium reduction from water to figure out its capability to be applied in wastewater treatment. A significant decrease in Cr concentration is seen after using CMC in the chromium containing solution near the WHO drinking water guideline which indicates its possible application for wastewater treatment. However, no adsorption kinetic model or chromium removal mechanism is reported here as this is only primary screening evidence representing the capability of CMC to remove residual chromium from water. Such adsorption model along with the practical deployment of water-soluble adsorbent is under investigation and will be reported in the next article. Nevertheless, due to chrome tanning process, tannery effluents of Bangladesh contain dangerously high level of chromium which is approximately 6000 times higher than the drinking water level and thus the the present investigation is only a preliminary indication of the application of CMC for tannery effluent treatment

Acknowledgement

The research work is mainly conducted in the 'Eco-friendly and Biodegradable Polymeric Materials Laboratory', Department of Materials Science and Engineering, Faculty of Engineering, University of Rajshahi, Rajshahi, Bangladesh-6205. The authors would like to thank the authorities of University of Rajshahi for providing facilities to carry out the research.

Funding Sources

The research was partially supported by the fund number A-1786/5/52/RU/Eng-12/2023-24 which was provided by the Faculty of Engineering, University of Rajshahi, Bangladesh-6205.

Conflict of Interest

The authors do not have any conflict of interest.

Data Availability Statement

The manuscript incorporates all datasets produced or examined throughout this research study.

Ethics Statement

This research did not involve human participants, animal subjects, or any material that requires ethical approval.

Informed Consent Statement

This study did not involve human participants, and therefore, informed consent was not required.

Permission to reproduce material from other sources

Not Applicable.

Author Contributions

- **Abu Mahmud:** Conceptualization, Investigation, Funding Acquisition, Methodology, Writing-Review & Editing, Software, Formal Analysis, Project Administration, Data Curation, Resources And Supervision.
- **Lila Dipto Joy:** Investigation, Methodology, Software, Writing - Original Draft, Formal Analysis.
- **Md. Habibul Islam:** Investigation.
- **Shamsad Sharmin:** Investigation, Resources.

References

1. Villamagna AM, Murphy BR. Ecological and socio-economic impacts of invasive water hyacinth (*Eichhornia crassipes*): a review. *Freshwater Biology*. 2010;55(2):282-298. doi:10.1111/j.1365-2427.2009.02294.x
2. Malik A. Environmental challenge vis a vis opportunity: The case of water hyacinth. *Environment International*. 2007;33(1):122-138. doi:10.1016/j.envint.2006.08.004
3. Rezania S, Ponraj M, Din MFM, Songip

AR, Sairan FM, Chelliapan S. The diverse applications of water hyacinth with main focus on sustainable energy and production for new era: An overview. *Renewable and Sustainable Energy Reviews*. 2015;41:943-954. doi:10.1016/j.rser.2014.09.006

4. Tanpichai S, Biswas SK, Witayakran S, Yano H. Water Hyacinth: A Sustainable Lignin-Poor Cellulose Source for the Production of Cellulose Nanofibers. *ACS Sustainable Chem Eng*. 2019;7(23):18884-18893. doi:10.1021/acssuschemeng.9b04095
5. Seddiqi H, Oliaei E, Honarkar H, *et al*. Cellulose and its derivatives: towards biomedical applications. *Cellulose*. 2021;28(4):1893-1931. doi:10.1007/s10570-020-03674-w
6. Klemm D, Heublein B, Fink HP, Bohn A. Cellulose: Fascinating Biopolymer and Sustainable Raw Material. *Angewandte Chemie International Edition*. Published online 2005. doi:10.1002/anie.200460587
7. Su JF, Huang Z, Yuan XY, Wang XY, Li M. Structure and properties of carboxymethyl cellulose/soy protein isolate blend edible films crosslinked by Maillard reactions. *Carbohydrate Polymers*. 2010;79(1):145-153. doi:10.1016/j.carbpol.2009.07.035
8. VanGinkel CG, Gayton S. The biodegradability and nontoxicity of carboxymethyl cellulose (DS 0.7) and intermediates. *Environmental Toxicology and Chemistry*. 1996;15(3):270-274. doi:10.1002/etc.5620150307
9. Mahmud Z, Manik MRK, Rahman A, Karim MM, Islam LN. Impact of untreated tannery wastewater in the evolution of multidrug-resistant bacteria in Bangladesh. *Sci Rep*. 2024;14(1):20379. doi:10.1038/s41598-024-71472-6
10. Shaibur MR. Extreme chromium enrichment in tannery-derived chrome cake: an overlooked environmental hazard. *Next Research*. 2026;7:101433. doi:10.1016/j.nexres.2026.101433
11. Nur-E-Alam Md, Mia MdAS, Ahmad F, Rahman MdM. An overview of chromium removal techniques from tannery effluent. *Appl Water Sci*. 2020;10(9):205. doi:10.1007/s13201-020-01286-0
12. Shaibur MR, Tanzia FKS, Nishi S, Nahar N, Parvin S, Adjadeh TA. Removal of Cr (VI) and Cu (II) from tannery effluent with water hyacinth and arum shoot powders: A study from Jashore, Bangladesh. *Journal of Hazardous Materials Advances*. 2022;7:100102. doi:10.1016/j.hazadv.2022.100102
13. Guidelines for Drinking-water Quality, Fourth Edition. Accessed March 15, 2026. https://www.who.int/docs/default-source/wash-documents/wash-chemicals/chromium-chemical-fact-sheet.pdf
14. Alemu A, Gabbiye N. Assessment of chromium contamination in the surface water and soil at the riparian of Abbay River caused by the nearby industries in Bahir Dar city, Ethiopia. *Water Practice and Technology*. 2017;12(1):72-79. doi:10.2166/wpt.2017.012
15. Sudarshan S, Harikrishnan S, RathiBhuvaneswari G, *et al*. Impact of textile dyes on human health and bioremediation of textile industry effluent using microorganisms: current status and future prospects. *Journal of Applied Microbiology*. 2023;134(2):lxac064. doi:10.1093/jambio/lxac064
16. Assefa H, Singh S, Olu FE, *et al*. Advances in adsorption technologies for hexavalent chromium removal: Mechanisms, materials, and optimization strategies. *Desalination and Water Treatment*. 2024;319:100576. doi:10.1016/j.dwt.2024.100576
17. Thepwat P, Saenchoopa A, Onnet W, *et al*. The synthesis and study of carboxymethyl cellulose from water hyacinth biomass stabilized silver nanoparticles for a colorimetric detection sensor of Hg(II) ions. *RSC Adv*. 2025;15(49):41241-41252. doi:10.1039/D5RA04757A
18. Nafi'ah R, Rosyidah S. Synthesis of Na-CMC Modified Cellulose Membrane From Water Hyacinth (Eichhornia Crassipes) Rods Against Cr (VI) Metal Adsorption. *JKPK*. 2021;6(3):352. doi:10.20961/jkpk.v6i3.55386
19. Prathima B, Srinivasa Raghvan V, Soni S, Gorthi SS, G.I. SB. Sulfide-enhanced carboxymethyl cellulose stabilised nano zero-valent iron for chromium(VI) mitigation in water: Evidence from batch and column studies. *Journal of Water Process Engineering*. 2024;66:105832. doi:10.1016/j.jwpe.2024.105832
20. Kukrety A. Comprehension on the Synthesis of Carboxymethylcellulose (CMC) Utilizing Various Cellulose Rich Waste Biomass

Resources. Waste Biomass Valor. 2018;9:1587-1595. doi:10.1007/s12649-017-9903-3

21. Tan L, Li H, Liu M. Characterization of CMC–LDH beads and their application in the removal of Cr(vi) from aqueous solution. *RSC Adv*. 8(23):12870-12878. doi:10.1039/c8ra00633d
22. Zhang X, Liu Z, Gao Y, Peng X, Shen W. Carboxymethyl cellulose enhanced Cr(VI) removal of zero-valent iron via the coating anti-passivation mechanism. *Journal of Water Process Engineering*. 2024;62:105321. doi:10.1016/j.jwpe.2024.105321
23. Worku Z, Tibebu S, Nure JF, *et al*. Adsorption of chromium from electroplating wastewater using activated carbon developed from water hyacinth. *BMC Chem*. 2023;17(1):85. doi:10.1186/s13065-023-00993-4
24. Agtasia Putri C, Yulianti I, Desianna I, Sholihah A, Sujarwata. Water hyacinth cellulose-based membrane for adsorption of liquid waste dyes and chromium. *J Phys: Conf Ser*. 2018;1008(1):012014. doi:10.1088/1742-6596/1008/1/012014
25. Pakutsah K, Aht-Ong D. Facile isolation of cellulose nanofibers from water hyacinth using water-based mechanical defibrillation: Insights into morphological, physical, and rheological properties. *International Journal of Biological Macromolecules*. 2020;145:64-76. doi:10.1016/j.ijbiomac.2019.12.172
26. Pushpamalar V, Langford SJ, Ahmad M, Lim YY. Optimization of reaction conditions for preparing carboxymethyl cellulose from sago waste. Carbohydr Polym. 2006;64(2):312-318. doi:10.1016/j.carbpol.2005.12.003
27. Adinugraha MP, Marseno DW, Haryadi. Synthesis and characterization of sodium carboxymethylcellulose from cavendish banana pseudo stem (Musa cavendishii LAMBERT). *Carbohydrate Polymers*. 2005;62(2):164-169. doi:10.1016/j.carbpol.2005.07.019
28. Albán Reyes DC, Gorzsás A, Stridh K, de Wit P, Sundman O. Alkalization of dissolving cellulose pulp with highly concentrated caustic at low NaOH stoichiometric excess. *Carbohydr Polym*. 2017;165:213-220. doi:10.1016/j.carbpol.2017.02.045
29. Salem KS, Kasera NK, Rahman MA, *et al*. Comparison and assessment of methods for cellulose crystallinity determination. *Chem Soc Rev*. 2023;52(18):6417-6446. doi:10.1039/D2CS00569G
30. Silva LE, dos Santos A de A, Torres L, *et al*. Redispersion and structural change evaluation of dried microfibrillated cellulose. *Carbohydrate Polymers*. 2021;252:117165. doi:10.1016/j.carbpol.2020.117165
31. *ASTM D1439-03(2008): Standard Test Method for Sodium Carboxymethylcellulose*. ASTM International; 2008. Accessed March 15, 2026. https://store.astm.org/d1439-03r08e01.html
32. Oh SY, Yoo DI, Shin Y, Seo G. FTIR analysis of cellulose treated with sodium hydroxide and carbon dioxide. *Carbohydrate Research*. 2005;340(3):417-428. doi:10.1016/j.carres.2004.11.027
33. Biswal DR, Singh RP. Characterisation of carboxymethyl cellulose and polyacrylamide graft copolymer. *Carbohydrate Polymers*. 2004;57(4):379-387. doi:10.1016/j.carbpol.2004.04.020
34. Johar N, Ahmad I, Dufresne A. Extraction, preparation and characterization of cellulose fibres and nanocrystals from rice husk. *Industrial Crops and Products*. 2012;37(1):93-99. doi:10.1016/j.indcrop.2011.12.016
35. French AD. Idealized powder diffraction patterns for cellulose polymorphs. *Cellulose*. 2014;21(2):885-896. doi:10.1007/s10570-013-0030-4
36. Trilokesh C, Uppuluri KB. Isolation and characterization of cellulose nanocrystals from jackfruit peel. *Sci Rep*. 2019;9(1):16709. doi:10.1038/s41598-019-53412-x
37. Poletto M. Thermal decomposition of wood: Influence of wood components and cellulose crystallite size. Bioresour Technol. 2012;109:148-153. doi:10.1016/j.biortech.2011.11.122
38. De Britto D, Assis OBG. Thermal degradation of carboxymethylcellulose in different salty forms. *Thermochimica Acta*. 2009;494(1-2):115-122. doi:10.1016/j.tca.2009.04.028
39. Mazlan MM, Kian LK, Fouad H, Jawaid M, Karim Z, Saba N. Synthesis and characterization of carboxymethyl cellulose from pineapple leaf and kenaf core biomass: a comparative study of new raw materials.

Biomass Conv Bioref. 2024;14(13):14653-14663. doi:10.1007/s13399-022-03700-w

40. Goldstein JI, Newbury DE, Michael JR, Ritchie NWM, Scott JHJ, Joy DC. Energy Dispersive X-ray Spectrometry: Physical Principles and User-Selected Parameters. In: Goldstein JI, Newbury DE, Michael JR, Ritchie NWM, Scott JHJ, Joy DC, eds. *Scanning Electron Microscopy and X-Ray Microanalysis*. Springer; 2018:209-234. doi:10.1007/978-1-4939-6676-9_16
41. Newbury DE, Ritchie NWM. Electron-Excited X-ray Microanalysis by Energy Dispersive Spectrometry at 50: Analytical Accuracy, Precision, Trace Sensitivity, and Quantitative Compositional Mapping. *Microsc Microanal*. 2019;25(5):1075-1105. doi:10.1017/S143192761901482X
42. Song L, Liu F, Zhu C, Li A. Facile one-step fabrication of carboxymethyl cellulose based hydrogel for highly efficient removal of Cr(VI) under mild acidic condition. *Chemical Engineering Journal*. 2019;369:641-651. doi:10.1016/j.cej.2019.03.126
43. Owlad M, Aroua MK, Daud WAW, Baroutian S. Removal of Hexavalent Chromium-Contaminated Water and Wastewater: A Review. *Water Air Soil Pollut*. 2009;200(1):59-77. doi:10.1007/s11270-008-9893-7
44. Lam B, Déon S, Morin-Crini N, Crini G, Fievet P. Polymer-enhanced ultrafiltration for heavy metal removal: Influence of chitosan and carboxymethyl cellulose on filtration performances. *Journal of Cleaner Production*. 2018;171:927-933. doi:10.1016/j.jclepro.2017.10.090
45. Szabó M, Kalmár J, Ditrói T, *et al*. Equilibria and kinetics of chromium(VI) speciation in aqueous solution – A comprehensive study from pH 2 to 11. *Inorganica Chimica Acta*. 2018;472:295-301. doi:10.1016/j.ica.2017.05.038
46. Zhao B, Gao B, Shi H, *et al*. In situ removal of Cr6+ with an intelligent adsorbent: Microwave synthesis, interface adsorption, thermodynamics, mechanism and self-regeneration. *Journal of Environmental Chemical Engineering*. 2024;12(2):112045. doi:10.1016/j.jece.2024.112045